

# Investigation of Power8 processors for astronomical adaptive optics real-time control

A. G. Basden,<sup>1\*</sup>

<sup>1</sup>*Department of Physics, South Road, Durham, DH1 3LE, UK*

27 May 2015

## ABSTRACT

The forthcoming Extremely Large Telescopes all require adaptive optics systems for their successful operation. The real-time control for these systems becomes computationally challenging, in part limited by the memory bandwidths required for wavefront reconstruction. We investigate new POWER8 processor technologies applied to the problem of real-time control for adaptive optics. These processors have a large memory bandwidth, and we show that they are suitable for operation of first-light ELT instrumentation, and propose some potential real-time control system designs. A CPU-based real-time control system significantly reduces complexity, improves maintainability, and leads to increased longevity for the real-time control system.

**Key words:** Instrumentation: adaptive optics, Instrumentation: miscellaneous, Methods: numerical.

## 1 INTRODUCTION

The forthcoming Extremely Large Telescopes (ELTs) (Spyromilio et al. 2008; Nelson & Sanders 2008; Johns 2008) will all rely on adaptive optics (AO) systems (Babcock 1953) for their successful operation, allowing the degrading effects of atmospheric turbulence to be greatly reduced. An AO system actively measures wavefront perturbations introduced by the Earth’s atmosphere, and attempts to mitigate these in real-time (on millisecond timescales) using one or more deformable mirrors (DMs). This is a computationally demanding task, and requires a dedicated real-time control system (RTCS). Computational requirements scale with the forth power of telescope diameter when considering traditional RTCS algorithms: for a given level of AO correction, the DM pitch must remain constant, and so the number of sub-apertures across the telescope pupil scales with telescope diameter,  $d$ . The total number of sub-apertures and actuators therefore each scale as  $\mathcal{O}(d^2)$ , and therefore the number of operations required for wavefront reconstruction (a matrix-vector multiplication) scales as  $\mathcal{O}(d^4)$ . Due to this rapid scaling of computational complexity, careful design considerations must be made when designing real-time control systems for the ELTs.

These RTCSs must be designed with long lifetimes, since the AO instruments on these telescopes are expected to be operational for at least thirty years (Vernet et al. 2012). Therefore maintenance, of both software and hardware is key to success. An RTCS design which is hardware ambigui-

ous, i.e. doesn’t require a particular hardware set to operate, is clearly advantageous. Previous system designs have frequently relied on specific hardware, typically digital signal processors (DSPs) and field programmable gate arrays (FPGAs) (for example the ESO SPARTA system, Fedrigo et al. 2006), which, due to long periods spent in design, are often close to obsolescence even during commissioning, with availability of spare parts becoming problematic, and specific programming knowledge required. Hardware failure of these systems then poses the risk that an entire new system will require designing, with the original software not being portable to new hardware.

In recent years, there has been much success with hardware agnostic AO RTCSs which operate on conventional PC hardware, including the Durham AO real-time controller (DARC) (Basden et al. 2010; Basden & Myers 2012), which is a generic system, used by the CANARY AO on-sky demonstrator instrument (Myers et al. 2008), and the real-time control system for the Gemini South telescope GeMS AO system (Rigaut et al. 2012). In theory, such systems simply require a recompilation of the source code to be ported to other (similar) hardware platforms, and are easy to move onto upgraded hardware. In practice, the advent of binary driver code, e.g. for wavefront sensors (WFSs) and DMs, means that porting is not always possible. Although porting to new hardware is typically limited to other PC-like systems that have an operating system running on a central processing unit (CPU), this is not always the case. In particular, the DARC system has a modular design which allows parts of the real-time pipeline to be placed in alternative hardware, including for example:

\* E-mail: a.g.basden@durham.ac.uk (AGB)

(i) pixel processing and slope calculation in FPGA using a customised version of the SPARTA system (Fedrigo et al. 2006)

(ii) wavefront reconstruction using graphics processing units (GPUs) (Basden et al. 2010)

(iii) a full GPU pipeline, from raw WFS images to DM demands.

However, this system still requires a CPU based core to oversee control of the hardware accelerators.

For ELT-scale AO systems, the largest computational requirements come from wavefront reconstruction algorithms, which typically use a matrix-vector multiplication (MVM) to obtain DM surface shape from WFS slope measurements. On conventional PC hardware, this algorithm is memory-bound, rather than compute-bound, and so for low latency operation, systems with large memory bandwidth are required. For this reason, accelerator cards (such as graphics processing units (GPUs)) are considered in designs for ELT-scale RTCs to provide the necessary memory bandwidths for these algorithms. However, this in itself raises new problems in moving data into and out of the accelerator for processing, which adds time and hence latency to the RTC pipeline. Designs that minimise this latency are key.

### 1.1 The POWER8 processor

The specification and road-map of the IBM POWER8 processor (Sinharoy et al. 2015) seems promising for AO RTCs, with two key relevant features: A memory bandwidth approaching that of GPUs (up to 230 GB/s), and support for a novel interconnect technology (NVLink, Foley 2014) due for release in 2017 that will provide an order of magnitude increase in data bandwidth between processor and GPU. Additionally, the OpenPower foundation has the potential for providing novel hardware acceleration architectures tightly coupled with POWER8 processors via the Coherent Accelerator Processor Interface (CAPI) (Stuecheli et al. 2015), including a currently available offering from the company Nallatech. The memory bandwidth of these processors is significantly larger than other available CPUs, hence the interest for AO real-time control, and a concise overview of the memory subsystems is given by Starke et al. (2015).

Here, we provide details of initial performance testing of the DARC RTCs on a POWER8 system.

In §2 we discuss the system configuration, RTC installation process and the tests that we perform. In §3 we present our findings, and we conclude in §4.

## 2 THE DARC REAL-TIME CONTROLLER ON A POWER8 SYSTEM

Most of the results that we will present here are performed on a low-end Tyan OpenPower Customer Reference system, model GN70-BP010, hosted at Durham. This system has a single 4-core POWER8 processor clocked at 3 GHz. Each core has 8-way symmetric multi-threading, providing a total of 32 hardware threads. The system has 16 GB DDR3 (1.6 GHz) RAM, controlled by a single Centaur memory controller. The total theoretical memory bandwidth for

this system is 28.8 GB/s between CPU and main memory (19.2 GB/s read, 9.6 GB/s write).

We have also had limited cloud access to a more powerful S824 POWER8 system with two 12-core processors (to which our machine instance had access to 22 cores), each 8-way threaded, providing a total of 176 hardware threads. Half of the memory banks of this machine are populated, and thus a total memory bandwidth of about 59 GB/s for read operations, and 29.5 GB/s for write operations is available. The operating system of this machine was run behind a hypervisor. Both of these systems run the Ubuntu operating system (14.10). Results presented here are from our low-end system unless stated otherwise.

### 2.1 Real-time control system installation

We use the publicly available DARC AO RTC system, with source code downloaded from the *sourceforge* hosting site. Installation on a POWER8 system was trivial: we simply had to remove three unsupported compiler options from the Makefile (`-msse2 -mfpmath=sse -march=native`) and then compile and install in the usual way. All of the required library dependencies were available from the Ubuntu repositories, and downloaded automatically as part of the DARC installation process. We did not attempt to optimise DARC using compiler flags specific to the POWER8 processor, and we used the freely available gcc compiler, for which source code is available (important for lifetime considerations).

We investigated the use of GigE Vision cameras for wavefront sensors, using the open-source Aravis library, with modifications specifically to allow access to the camera pixel stream, rather than full-frame access (to reduce RTC latency). Because this library is entirely open-source, and does not require any hardware drivers, there were no issues with binary drivers. This library provides access to a number of wavefront sensors that have been used on-sky with the CANARY AO system, including an Imperx Bobcat camera, an Emergent Vision Technologies HS2000 10Gbit camera and a First-Light OCAM2S camera. During operation, as soon as sufficient pixels have arrived at the computer to complete a given sub-aperture, this sub-aperture is processed by a thread (calibration, slope calculation and partial reconstruction). The thread then returns to compute the next available sub-aperture, in a round-robin fashion. Once all sub-apertures for a given frame have been processed, each thread will have a partial DM vector, and these are then combined in a reduction step to yield the final DM command.

To further demonstrate the proof of concept of a complete AO system, we selected an Alpao 241 actuator DM with an Ethernet interface. It was necessary to develop our own library interface for this DM since source code for the Software Developers Kit was not available, and the binary libraries were for X86 architectures. However, control of this DM involves sending a UDP packet, and so was trivial to implement. A closed-loop AO system driven by a POWER8 server is therefore feasible using an existing RTCs.

## 2.2 Testing real-time performance

We investigate the performance of DARC on POWER8 by configuring the system as would be used in a number of different AO cases. These are:

- (i) A  $40 \times 40$  sub-aperture single conjugate AO (SCAO) system.
- (ii) A  $80 \times 80$  sub-aperture SCAO system.
- (iii) A  $80 \times 80$  sub-aperture system with increased actuator counts.

For each of these cases, we investigate performance for different sized sub-apertures, i.e. different numbers of pixels per sub-aperture.

The third case can be viewed as a single WFS of the proposed European ELT (E-ELT) multi-conjugate adaptive optics (MCAO) instrument (Foppiani et al. 2010) with computation of a full set of partial DM demands. A full MCAO real-time control system could then be comprised of one compute node per WFS, with combination of partial DM demands being computed as a (low operation count) final processing step to give the demands to be sent to the DMs. We discuss this further in §3.4

Our tests presented here do not include a physical WFS camera or DM, since we do not have suitable equipment available (specifically, cameras with sufficient pixels and frame-rates, and a DM with enough actuators). Rather, we concentrate on the core computational pipeline. Our previous experience has shown that introducing a physical camera to a system has little impact on overall performance (maximum achievable frame rate), provided the camera itself is capable of reaching these frame rates. Because the DARC RTCS can process pixels as they arrive at the computer, then once the last pixel for a given frame arrives, most of the computation has typically already completed. The RTCS is used without frame pipe-lining here, i.e. there are never two frames being processed at once, so that the frame-rate represents the computation time of a given frame. We note that with a real camera, expected readout time and data transfer time will depend very much on camera model, and in astronomical AO the readout time is often the limiting factor in achievable frame-rate (likely to be the case for the forthcoming ELTs), and for true latency considerations, this should be taken into account. For example, for a camera with a maximum frame rate of 500 Hz, the readout time (and exposure time) will be 2 ms. Assuming that data is transferred as it is read out (rather than buffered), this means there will be a delay of 4 ms from start of exposure to last pixel arriving at the computer (by which time, most of the computation will have completed). However, an investigation of camera latency is beyond the scope of this paper.

Of key importance in the approach that we take is that we are using a fully configured AO RTCS, which has been proven on-sky. When bench-marking hardware performance, it can be tempting to write simple bench-marking code which investigates the key algorithms under consideration, i.e. image calibration (vector operations), slope computation (vector and reduction operations), and wavefront reconstruction (matrix-vector multiplication). However, this leads to optimistic performance estimates, since the benchmark is grossly simplified and bears little resemblance to actual code that would be usable on-sky at a telescope.

### 2.2.1 The performance metric

We define the performance of the RTCS by measuring the time taken to perform the computation for each AO system frame. In the default DARC configuration, which we use here, the computation of each frame must be completed before the next frame is started. This therefore means that the inverse of the frame computation time gives the maximum achievable frame-rate for the AO system. This behaviour is critical for optimising AO system latency on a given hardware set.

The DARC RTCS uses a horizontal processing strategy (Basden et al. 2010) with each thread operating on WFS data from start to finish, rather than having different threads performing individual tasks (e.g. a set of threads for image calibration, a set for slope computation, and a set for wavefront reconstruction). This strategy allows automatic load balancing by the operating system, and simplifies performance optimisation: the main parameter to be optimised is the number of processing threads, rather than balancing the number of threads per algorithm which can become a complex optimisation problem. Of further consideration is the number of sub-apertures that each thread should process at once, influencing the order of memory operations and the size of the partial matrix-vector multiplications. If this is too small, then many inefficient small matrix-vector multiplication operations will reduce the performance, while if too large, a small number of large matrix-vector multiplication operations will lead to a saturation of memory bandwidth, resulting in threads being work-starved.

## 2.3 Tests of memory bandwidth

To directly test the memory bandwidth available, we use the STREAM benchmark (McCalpin 1995), which performs a number of different memory read and write operations. Results are given in table 1, and show that for our low-end (4-core) server, over 85% of theoretical memory bandwidth can be reached, while achieving nearly 80% on the higher-end machine. There are several things to note here: we did not optimise the STREAM benchmark on the higher-end machine due to limited access, and so actual performance is expected to be slightly higher. The STREAM results include memory read and write access, which will lead to lower than expected results for some of these tests since the available bandwidth on POWER8 systems is asymmetric (i.e. the read bandwidth is twice the write bandwidth). A non-standard read-only version of Triad shows slightly higher memory bandwidth utilisation, reaching 90.9% of the theoretical maximum.

## 3 RTCS PERFORMANCE ON POWER8

We now consider the achievable performance on the POWER8 systems under investigation, and consider the application for future RTCS designs. For each case, we investigate changing the number of threads used by DARC, and the processing block size used, i.e. the number of sub-apertures processed together as a block.

STREAM Function	GB/s (4-core machine)	GB/s (22-core machine)
Copy	15.5	46.0
Scale	15.1	45.5
Add	16.3	41.0
Triad	16.4	46.1
Read-only Triad	17.4	

**Table 1.** The STREAM benchmark results for the POWER8 systems under investigation here (total memory bandwidth achieved). For the 4-core machine, best performance was using 3 threads, while 48 threads were used for the 22-core machine. The Read-only line is an additional function that we added to test read memory access only (i.e. no memory writes are performed), and is achieved using 4 threads.

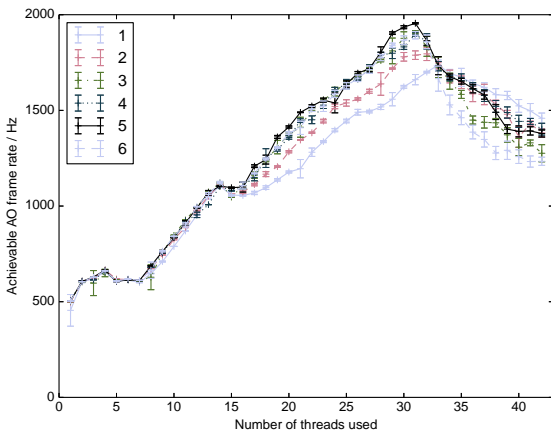


**Figure 1.** Achievable RTCS frame rate as a function of number of processing threads used. The individual lines represent the number of times (given by the legend) threads are reused each frame (affecting the number of partial matrix-vector products that are implemented).

### 3.1 An 8 m XAO system

We investigate the case of a eXtreme AO (XAO) system on an 8 m telescope with 20 cm sub-apertures ( $40 \times 40$ ), and results are shown in Fig. 1. Here, it can be seen that with the low-end system a maximum frame-rate of nearly 2 kHz is achieved. In this case, the control matrix size is  $1304 \times 2480$ , requiring a memory bandwidth of 23.4 GB/s to read this from main memory every RTCS iteration at this frame rate. This is larger than the available memory bandwidth (19.2 GB/s) and therefore, the control matrix (12 MB) is being stored in the large L3 cache (32 MB).

RTCS processing tasks are divided among a selected number of threads, and we see that using 31 threads provides best performance. The processor has 4 cores, each with 8-way simultaneous multithreading capability (i.e. 32 virtual cores). Of particular note is the linearity of these curves between 8 threads and the peak: the RTCS pipeline is seen to be highly parallelisable with performance scaling almost directly with the number of cores available.

We also consider the case when this system has a larger number of actuators to control, e.g. for a woofer-tweeter system. This is of particular interest, because it will allow us to measure maximum RTCS performance as the control matrix

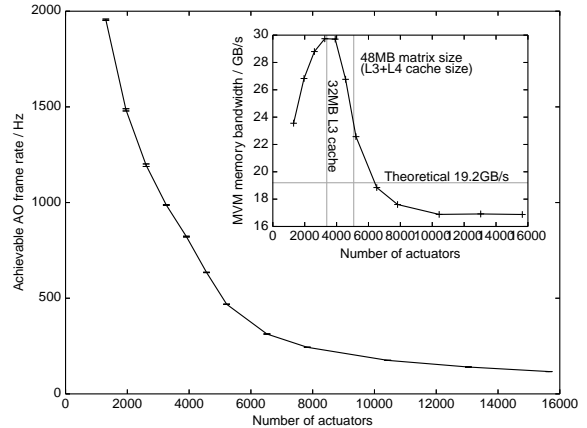


**Figure 2.** Maximum achievable RTCS frame rate as a function of number of actuators controlled for a  $40 \times 40$  sub-aperture system. Inset is shown the corresponding memory bandwidth required by the matrix-vector multiplication to achieve this frame rate.

size approaches, and exceeds, that of the L3 cache. Fig. 2 shows these results (with the optimum number of processing threads selected), which shows an expected degradation of achievable AO frame rate as the problem size increases. Once the control matrix size approaches about 48 MB (equal to the size of the L3 and L4 cache combined), then performance is clearly degraded, with memory bandwidth between the processor and main memory becoming the limiting factor. Performance levels off utilising about 90% of the available memory bandwidth for large control matrix sizes, in agreement with the STREAM benchmark.

### 3.2 A single ELT WFS

We investigate the case of an E-ELT single conjugate AO (SCAO) system, with a single WFS with  $80 \times 80$  sub-apertures (with  $6 \times 6$  pixels per sub-aperture), and a control matrix of size  $5160 \times 9824$  (193 MB). In this case, the maximum frame rate is 100.2 Hz on our low-end system, requiring a memory bandwidth of 18.9 GB/s to read the matrix from memory each iteration (it is too large to fit in cache), in addition to reading calibration image and other memory operations. This is very close to the theoretical maximum memory bandwidth, and so we conclude that the POWER8 architecture is optimised and pipelined in such a way as to achieve peak performance for mixed processing tasks.

The higher-end system provides a maximum frame-rate of 150 Hz, requiring a memory bandwidth of 28.8 GB/s (with a slightly larger control matrix with 10,000 actuators). It should be noted that because of the way the RTCS is currently implemented, a single copy of the control matrix is accessed, and therefore will be stored in the memory attached to one processor. Threads executing on the second processor must therefore access this matrix via the first processor, therefore limiting the available memory bandwidth for control matrix access to that of one processor, i.e. 29.5 GB/s in this case. This is clearly a limiting factor for the RTCS, in part due to the non-uniform memory access (NUMA) architecture of the multi-processor computer hardware, one

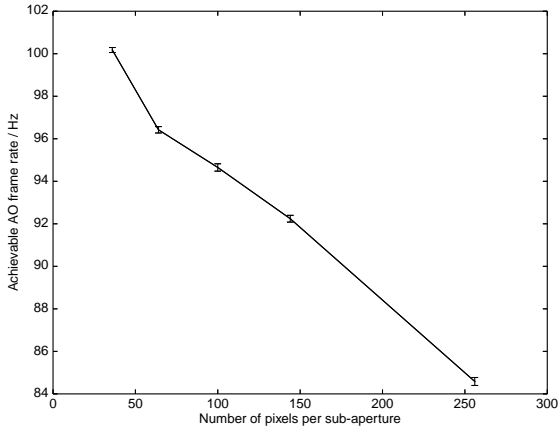


**Figure 3.** Maximum AO frame rate as a function of number of pixels per sub-aperture (with  $80 \times 80$  square sub-apertures).

which is now on the list of improvements to be made to the DARC system. We note here that we are achieving an effective memory bandwidth very close to the theoretical limit available to the system.

For reference a top-end Intel X86 processor (E5-2699-v3) has 18 cores and a 45 MB level-3 cache, with 68 GB/s access to main system memory, costing around 5000.

We also investigate the effect of number of pixels on AO real-time performance, with Fig. 3 showing maximum AO frame rate on our low-end POWER8 hardware as a function of number of pixels per sub-aperture. Increasing the number of pixels per sub-aperture reduces maximum frame-rate, suggesting that as sub-apertures get larger, the matrix-vector multiplication is no longer the sole rate limiting factor. Although the memory bandwidth required to read an image, background map and flat-field information at the AO frame rate is small (compared to that required for the control matrix), at only 1.5 GB/s for the largest sub-apertures used here, the larger images will have a larger impact on cache operations, meaning that less of the control matrix is available in cache for when required, leading to additional memory reads, and reduced AO frame-rates. Additionally, a larger number of floating point operations are required for pixel processing, meaning that the matrix-vector multiplication time is no longer so dominant.

### 3.2.1 Thread counts

We investigate how the number of processing threads affects the achievable AO frame rate. Fig. 4 shows that using close to, but less than, the number of hardware threads (32) provides best performance. Of particular note here is that (in comparison with Fig. 1) performance no longer scales directly with the number of processing cores. This is because this larger problem size is memory bandwidth limited, rather than compute limited.

### 3.2.2 Amdahl's law

Amdahl's law (Amdahl 1967) states that the performance gain in a system through parallelisation (or other) tech-

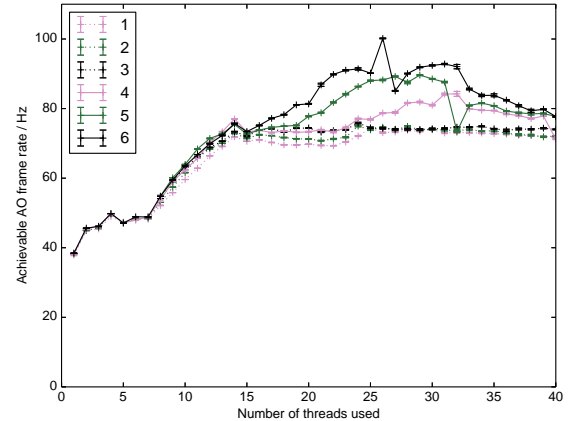


**Figure 4.** A figure showing how maximum achievable AO frame rate is dependent on the number of processing threads used. The individual lines represent the number of times (given by the legend) threads are reused each frame.

niques is limited by the fraction of time spent within the parts of the system benefiting from those improvements.

In the case of a high order AO RTCS, the limiting performance factor is memory bandwidth, required for wavefront reconstruction. Increasing available memory bandwidth will only continue to significantly improve performance while other parts of the computational pipeline (namely image calibration and slope calculation) do not begin to dominate the computation time. Therefore, to be able to make scaled performance predictions, we need to be able to determine the time taken for these operations which are compute limited rather than memory bandwidth limited.

We therefore investigate performance with and without wavefront reconstruction. For the case without wavefront reconstruction, we are interested in how well the POWER8 system can process pixel information and produce wavefront slopes, and assume that the reconstruction could be performed elsewhere (i.e. in a GPU, using NVLink), though of course this may introduce additional latency.

Fig. 5 shows maximum achievable frame rates for the AO RTCS processing pipeline when the large matrix-vector multiplication for wavefront reconstruction is removed, and thus places an approximate limit on achievable performance for these processors when unlimited memory bandwidth is available. Therefore, we can see that when using a POWER8 system with greater memory bandwidth (up to 256 GB/s read bandwidth for a dual-processor server), frame rates of nearly 1.3 kHz should be available for this system, limited by the memory bandwidth for wavefront reconstruction, since we know that other aspects of the real-time pipeline can be performed faster than this (1.6 kHz on our low-end system, and faster on a high end 24-core server).

## 3.3 A multiple mirror ELT SCAO system

To investigate the performance of this ELT-scale SCAO system further, we consider the case of multiple mirror SCAO systems, i.e. with an increased number of actuators. This increases the control matrix size, and thus allows us to inves-

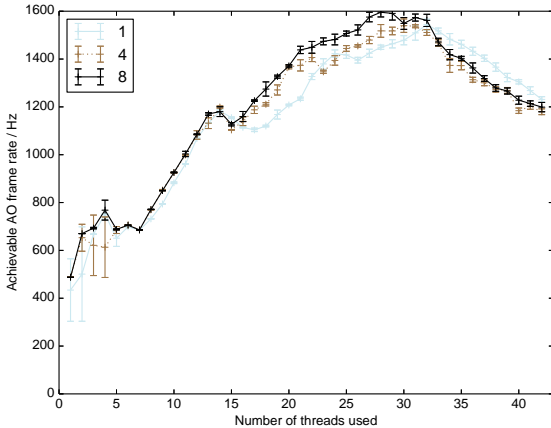


**Figure 5.** A figure showing achievable AO RTCS frame-rates as a function of thread count on the low-end POWER8 system when wavefront reconstruction is not performed, for an ELT-scale SCAO system ( $80 \times 80$  sub-apertures).

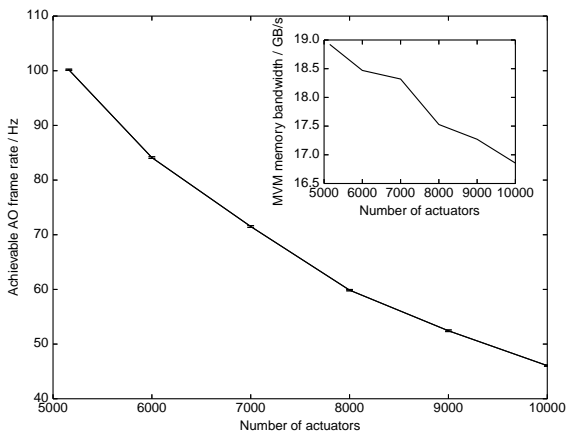


**Figure 6.** Maximum AO frame rate as a function of number of actuators controlled with  $80 \times 80$  sub-apertures. Inset is shown the memory bandwidth required reach this frame rate for a given matrix size.

tigate performance limiting factors for different AO system configurations. We also investigate performance with different sub-aperture sizes (pixels per sub-aperture), so that we can separate compute intensive and memory intensive tasks.

Fig. 6 shows maximum AO frame rate on our low-end POWER8 hardware as a function of control matrix size.

The maximum achievable frame-rate is reduced proportionally to the control matrix size, again limited by memory bandwidth, though we see that for larger matrices, the memory bandwidth achieved is slightly reduced. We believe that this is due to less of the larger matrix being cached, i.e. when there is a larger matrix to read, cache prediction is not so good. However, the system is still able to achieve nearly 90% of theoretical memory bandwidth during the AO system loop.

### 3.3.1 Operation at necessary frame rates

The maximum frame rates reported so far have not been sufficient for an on-sky ELT AO system. However, we have only been able to perform bench marking on a low-end system. Due to the high utilisation of available memory bandwidth (close to 100%), we can make predictions as to maximum achievable frame rates for currently available higher end systems. A POWER8 S824 system contains two processors, each with up to 128 GB/s memory bandwidth for read operations, a combined factor of 13.3 times greater than our system. If memory bandwidth is the limiting factor, we could expect an AO frame rate of greater than 1.2 kHz for an ELT-scale SCAO system using an S824 system. It is likely that other parts of the computational pipeline would start to limit performance so that this frame rate would not be achieved. In §3.2.2 we have investigated performance on our low-end system with the matrix-vector multiplication removed, to demonstrate that pixel processing and slope computation at higher frame rates is achievable. Therefore, with sufficient memory bandwidth, ELT frame rates are easily available on an existing POWER8 server.

### 3.4 An ELT MCAO system

We have considered the performance case for an ELT-scale SCAO system, and we now use this information to consider MCAO system design. The E-ELT MCAO instrument, MAORY (Foppiani et al. 2010), is likely to have 4–6 laser guide stars (LGSs) and up to 3 natural guide star (NGS) low order wavefront sensors, with a total of 2 or 3 DMs (including the telescope M4 DM), operating up to 10,000 actuators with a 500 Hz frame rate.

Processing of WFS images to yield wavefront gradients is independent, i.e. slopes obtained by processing one WFS do not depend on the processing of other WFSs. Similarly, when using conventional matrix-vector multiplication wavefront reconstruction methods (we discuss other methods in §3.7, the slopes from each WFS can be used independently of other WFSs to compute a partial set of DM commands. The partial DM commands from each WFS can then be summed, yielding the final DM demands to be applied to the mirror, in a low count vector addition operation.

We therefore now consider a MCAO control solution which has a separate POWER8 server for each LGS WFS (directly connected), and an additional POWER8 server for the three NGS, with partial DM demands being sent to one server for summation to yield the final DM demands, as shown in Fig. 7. We note that since the NGS are likely to be of lower order (resulting in a smaller matrix-vector multiplication), it would be possible to process all NGS in a single server, reducing cost and complexity. This server is then also used to collate the partial DM demands, which will arrive over more than one 10G Ethernet link to reduce latency.

With this control solution, each server therefore has to process a single WFS, and between 8000–10000 actuators, and so we can directly estimate expected performance using Fig. 3, which by scaling to the memory bandwidth available in a S824 system, will yield frame rates above 500 Hz, the MAORY design goal. Further processor improvements over the next few years (for example the Power9 processor in

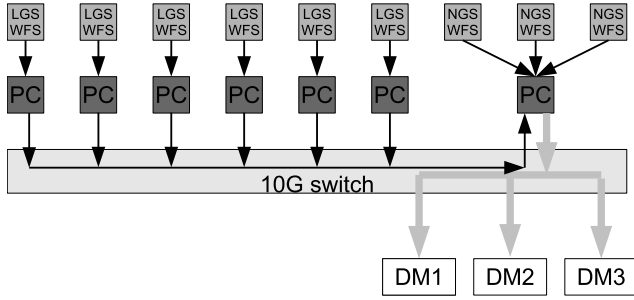


**Figure 7.** A schematic design showing components for a ELT MCAO real-time control system, and the links between them. WFSs are connected individually to a POWER8 server, which computes partial DM demands. These are then summed before being sent to the DM.

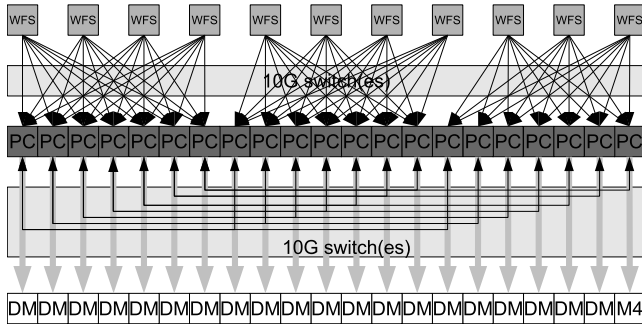


**Figure 8.** A schematic design showing components for a ELT MOAO real-time control system, and the links between them. Four WFSs are connected to a server, which computes slope measurements, and shares these with two other servers. Each server then has access to all wavefront sensor slope measurements, and computes DM demands for a single DM.

2017) will improve performance further, and be available within the time frame of MAORY system development.

### 3.5 An ELT MOAO system

We now consider requirements for an ELT-scale multi-object AO (MOAO) system. The E-ELT MOAO instrument is likely to be MOSAIC (Hammer et al. 2014), and will use 6 LGS and up to 5 NGS. Up to 20 MOAO channels are proposed, each with a DM, in addition to the main telescope M4 deformable mirror.

Fig. 8 shows a possible schematic design for the MOAO real-time control system. In summary, 21 servers are required, one for each DM, including the M4 mirror. Each server receives images from 3 or 4 WFSs and processes these to provide wavefront slope information. These wavefront slopes are then shared with two other servers, which in return also share the wavefront slope information computed from their WFSs. Therefore, each server will have access to the 11 WFS slope vectors. Each server then performs a tomographic wavefront reconstruction, projected along a given line of sight, and sends the DM demands to the relevant DM.

With this design, each server is responsible for process-

ing 4 WFS images, and performing a matrix-vector multiplication with a matrix size of about  $100,000 \times 5000$ . At the desired frame rate of 250 Hz, this represents a required memory bandwidth of about 470 GB/s, which is achievable using a 4-socket POWER8 server (e.g. the S850 system, which has a read memory bandwidth of 512 GB/s), though is likely that within the next decade (the time-frame for ELT MOAO instrument development), significant improvements in memory bandwidth will be realised, enabling this performance goal to be met with even greater overhead, reducing latency. Additionally, the inclusion of one or two GPUs to the system (taking advantage of the forthcoming high performance NVLINK interconnect, Foley 2014) specifically to perform matrix-vector multiplication would further reduce latency. We discuss this further in §3.7.

It should be noted that with this design, the wavefront reconstruction for each DM is independent, allowing different algorithms to be trialled with performance comparisons made while the system is in operation. This capability will be key to maximising MOAO performance.

### 3.6 Variation in latency

The variation of AO system latency, or jitter, is a key parameter when developing a real-time control system. If this jitter is large, then there will be frequent delays in the AO processing pipeline, leading to reduced AO performance. This is particularly critical for higher order AO systems. Fig. 9 shows the variation in latency measured over 1,000,000 frames on the POWER8 server for both the  $40 \times 40$  and  $80 \times 80$  sub-aperture systems. For the higher order case, the variation in latency follows a Gaussian distribution, with a FWHM of 1.4 ms, 5% of the mean frame time. No frames take more than twice the mean frame time, and 99% of frames take less than 8% longer than the mean time.

For the low order case, the variation in latency is no longer Gaussian, showing an extended tail, and additional features that may be related to the granularity of the timer. The rms jitter is  $62\mu\text{s}$ . Here, less than 0.01% of frames take longer than twice the mean frame time to complete, and 99% of frames take less than 38% longer than the mean frame time to complete.

We are currently using a stock Ubuntu kernel (3.16.0-23). The use of a real-time kernel would further improve this jitter, though we do not investigate here as this is not yet available.

### 3.7 Further considerations

We have so far only considered the basic AO RTCS pipeline operations, including wavefront reconstruction using a matrix-vector multiplication algorithm, image calibration and slope computation. However, for an ELT, this is unlikely to be sufficient, as further algorithms will be necessary, for example the linear-quadratic-gaussian (LQG) control as demonstrated by CANARY, for vibration mitigation (Sivo et al. 2014), which involves several matrix-vector multiplication operations.

Current implementations of LQG demonstrated on-sky have required significantly more computational power and



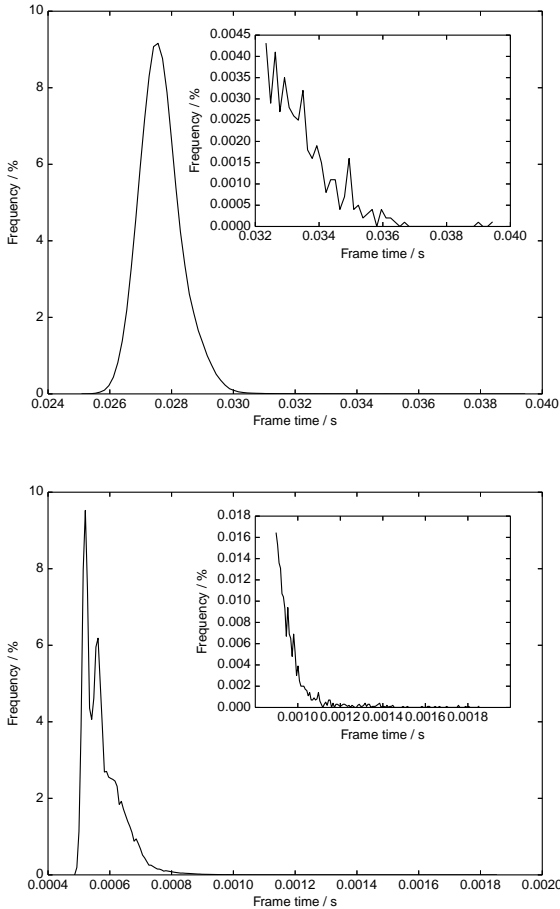


**Figure 9.** (a) A histogram of frame computation times for an  $80 \times 80$  SCAO system. (b) A histogram of frame computation times for a  $40 \times 40$  SCAO system.

memory bandwidth than a conventional matrix-vector multiplication algorithm, and so the hardware that we are investigating here may not be sufficient for these algorithms. There are two alternatives: LQG is an active area of research, and efficient implementations are being developed (Gray & Le Roux 2012). Alternatively, hardware acceleration techniques can be considered.

A requirement for additional hardware acceleration will benefit significantly from the proposed high-speed NVLINK and CAPI interconnects under development for future POWER8 processors and hardware accelerators. Specific hardware, for example GPUs or FPGAs, can be used to provide acceleration of given algorithms, in this case, the wavefront reconstruction problem. A high-speed, low latency link is key to enabling this, as it will maintain low system latency: improved algorithmic behaviour will only improve AO system performance if the algorithms do not lead to significant increases in AO system latency. A key feature of the CAPI interface is that it enables abstracted code to be developed with accelerators sharing the same memory address space as the CPU, allowing code to be developed independently of the physical hardware acceleration used.

A high bandwidth, low latency accelerator interconnect

is also essential for future designs of ELT-scale XAO real-time systems. For these systems, low latency is critical.

### 3.7.1 Future-proofing AO real-time control

We have demonstrated that an existing AO RTCS can be ported to an alternative processor technology with very little effort, and that this technology has the potential to enable AO real-time control for first-light ELT AO instruments without the requirement for additional hardware acceleration. This greatly simplifies RTCS design, and provides greater confidence that the RTCS software will be able to operate for the foreseeable future, independent of underlying hardware changes (provided a C compiler exists). No proprietary libraries are necessary, and full source code for this system is available.

Of key importance here is that an ELT-scale AO real-time control system can be developed in the widely used C programming language, and does not require any custom hardware, or any niche untransferable skills. Transferability of this system to other processor types give a significant degree of confidence that a system developed in this way will remain operable, configurable, upgradable and hardware independent for the foreseeable future. This is a key advantage for telescopes with expected operational lifetimes approaching a century.

## 4 CONCLUSION

We have investigated the use of a freely available, open source, AO RTCS on new POWER8 hardware. We find that installation on this hardware was trivial, demonstrated the use of WFSs and a DM, and find that computational performance is in line with expectations, with ELT-scale AO RTCS performance being limited by available memory bandwidth, of which our RTCS typically reaches above 90% of the theoretical maximum. The large potential memory bandwidth of the POWER8 CPU, along with forthcoming innovations enabling high bandwidth communication between the CPU and other hardware (including GPUs, with NVLink), means that POWER8 systems are a prime contender for use with ELT-scale AO RTCSs, and that using conventional computer server technology is highly attractive to maintain longevity, upgradability and comprehension of these systems.

## ACKNOWLEDGEMENTS

This work is funded by the UK Science and Technology Facilities Council, grant ST/K003569/1. We thank the referee who helped improve this paper.

## REFERENCES

- Amdahl G., 1967, in AFIPS Conference Proceedings, Volume 30, pp. 483-485 (1967) Validity of the Single Processor Approach to Achieving Large-Scale Computing Capabilities. pp 483-485
- Babcock H. W., 1953, Pub. Astron. Soc. Pacific, 65, 229



- Basden A., Geng D., Myers R., Younger E., 2010, *Appl. Optics*, 49, 6354
- Basden A. G., Myers R. M., 2012, *MNRAS*, 424, 1483
- Fedrico E., Donaldson R., Soenke C., Myers R., Goodsell S., Geng D., Saunter C., Dipper N., 2006, in *Advances in Adaptive Optics II*. Edited by Ellerbroek, Brent L.; Bonaccini Calia, Domenico. *Proceedings of the SPIE*, Volume 6272, pp. 627210 (2006). Vol. 6272 of Presented at the Society of Photo-Optical Instrumentation Engineers (SPIE) Conference, SPARTA: the ESO standard platform for adaptive optics real time applications
- Foley D., 2014, Technical report, NVLink, Pascal and Stacked Memory: Feeding the Appetite for Big Data, <http://devblogs.nvidia.com/parallelforall/nvlink-pascal-stacked-memory-feeding-appetite-big-data/>
- NVIDIA
- Foppiani I., Diolaiti E., Baruffolo A., Biliotti V., Bregoli G., Cosentino G., Delabre B., Lombini M., Marchetti E., Rossetini P., Schreiber L., Tomelleri R., Conan J.-M., D’Odorico S., Hubin N., 2010, in *Society of Photo-Optical Instrumentation Engineers (SPIE) Conference Series* Vol. 7736 of *Society of Photo-Optical Instrumentation Engineers (SPIE) Conference Series*, System overview of the Multi conjugated Adaptive Optics RelaY for the E-ELT
- Gray M., Le Roux B., , 2012, Ensemble Transform Kalman Filter, a nonstationary control law for complex AO systems on ELTs: theoretical aspects and first simulations results
- Hammer F., Barbuy B., Cuby J., Kaper L., Morris S., Evans C., Jagourel P., Puech M., 2014, in *Society of Photo-Optical Instrumentation Engineers (SPIE) Conference Series* Vol. in print of *Society of Photo-Optical Instrumentation Engineers (SPIE) Conference Series*, MO-SAIC at E-ELT: a MOS for astrophysics, IGM, and cosmology
- Johns M., 2008, in *Extremely Large Telescopes: Which Wavelengths? Retirement Symposium for Arne Ardeberg* Vol. 6986, *The giant magellan telescope (gmt)*. pp 698603–698603–12
- McCalpin J. D., 1995, *IEEE Computer Society Technical Committee on Computer Architecture (TCCA) Newsletter*, 12, 19
- Myers R. M., Hubert Z., Morris T. J., Gendron E., Dipper N. A., Kellerer A., Goodsell S. J., Rousset G., Younger E., Marteaud M., Basden A. G., 2008, in *Society of Photo-Optical Instrumentation Engineers (SPIE) Conference Series* Vol. 7015 of Presented at the Society of Photo-Optical Instrumentation Engineers (SPIE) Conference, CANARY: the on-sky NGS/LGS MOAO demonstrator for EAGLE
- Nelson J., Sanders G. H., 2008, in *Society of Photo-Optical Instrumentation Engineers (SPIE) Conference Series* Vol. 7012 of *Society of Photo-Optical Instrumentation Engineers (SPIE) Conference Series*, The status of the Thirty Meter Telescope project. pp 70121A–70121A–18
- Rigaut F., Neichel B., Boccas M., d’Orgeville C., Arriagada G., Fesquet V., Diggs S. J., Marchant C., Gausach G., Rambold W. N., Luhrs J., Walker S., Carrasco-Damele E. R., Edwards M. L., Pessev P., Galvez R. L., 2012, in *Society of Photo-Optical Instrumentation Engineers (SPIE) Conference Series* Vol. 8447 of *Society of Photo-Optical Instrumentation Engineers (SPIE) Conference Series*, GeMS: first on-sky results
- Sinharoy B., Van Norstrand J. A., Eickemeyer R. J., Le H. Q., Leenstra J., Nguyen D. Q., Konigsburg B., 2015, *IBM Journal of Research and Development*, 59, 2:2
- Sivo G., Kulcsar C., Conan J., Raynaud H., Gendron E., Basden A., Vidal F., Morris T., 2014, *Opt. Express*
- Spyromilio J., Comerón F., D’Odorico S., Kissler-Patig M., Gilmozzi R., 2008, *The Messenger*, 133, 2
- Starke W. J., Stuecheli J., Daly D., Dodson J., Auernhammer F., Sagmeister P. M., Guthrie G. L., Marino C. F., Siegel M., Blaner B., 2015, *IBM Journal of Research and Development*, 59(1), 3:1
- Stacked Memory Feeding Appetite for Big Data, 2015, *IBM Journal of Research and Development*, 59, 7:1
- Vernet E., Cayrel M., Hubin N., Mueller M., Biasi R., Gallieni D., Tintori M., , 2012, Specifications and design of the E-ELT M4 adaptive unit

This paper has been typeset from a  $\text{\TeX}$ / $\text{\LaTeX}$  file prepared by the author.